Electronic Supplementary Material (ESI) for Nanoscale.

Bright Monolayer Tungsten Disulfide *via* Exciton and Trion Chemical Modulations

Ye Tao,[‡, a] *Xuechao Yu,*[‡, a] *Jiewei Li,*[b] *Houkun Liang,*[c] *Ying Zhang,*[c] *Wei Huang*[b, d] *and Qi Jie Wang*[*, a]

[a] Centre for OptoElectronics and Biophotonics, School of Electrical and Electronic Engineering & The Photonics Institute, Nanyang Technological University, 50 Nanyang Avenue, 639798, Singapore

[b] Key Laboratory of Flexible Electronics & Institute of Advanced Materials, Jiangsu National Synergetic Innovation Center for Advanced Materials, Nanjing Tech University, 30 South Puzhu Road, Nanjing 211816, China

[c] Singapore Institute of Manufacturing Technology, 71 Nanyang Drive, 638075 Singapore

[d] Key Laboratory for Organic Electronics and Information Displays & Institute of Advanced Materials, Jiangsu National Synergetic Innovation Center for Advanced Materials, Nanjing University of Posts & Telecommunications, 9 Wenyuan Road, Nanjing 210023, China

1. Optical properties

The photoluminescence (PL) spectra of monolayer WS_2 on SiO_2/Si substrate were conducted through a WITec alpha 300 R system with excitation wavelength of 532 nm at room temperature. In order to avoid heating and optical doping effect, the power of laser was kept as low as 7 μW for the room temperature PL measurement and 30 μW for the low temperature (77 K) circularly polarized PL measurement, respectively. The linear polarizer and quarter-wave plate were used for the measurement of circularly polarized PL spectra.

The pristine monolayer WS_2 shows a wide PL spectrum with an emission peak at ~1.99 eV, which is arising from both neutral exciton and electron bonded trion. In contrast, the PL spectra of the HATCN doped monolayer WS_2 become sharp and blue shift with an emission peak at ~2.02 eV, which is due to the transition from the trion to exciton through electron transfer from monolayer WS_2 to HATCN.

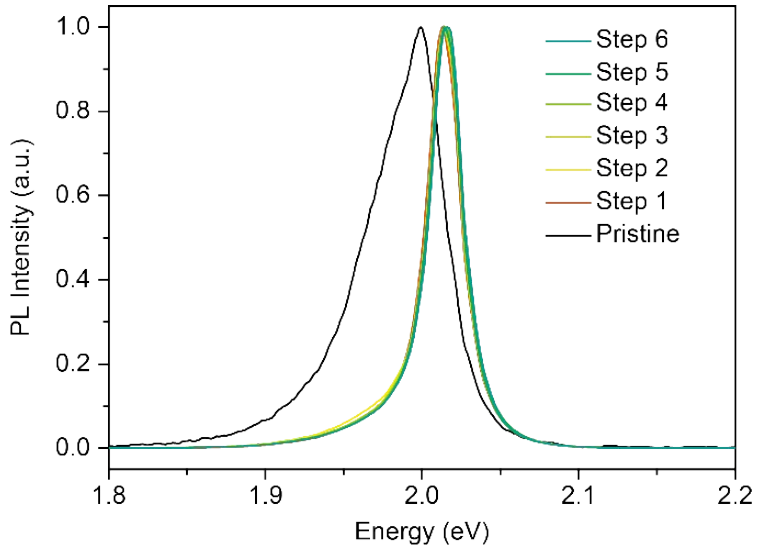

Figure S1. Normalized PL spectra of pristine and HATCN doped monolayer WS_2.

The non-uniformity intensity of the PL mapping may be due to the variation of natural doping (n doping) in pristine monolayer WS_2. The uneven distribution of natural doping could result in different formation possibility of electron bounded trion (low PL intensity) and neutral exciton (high PL intensity) in the different area of monolayer WS_2. As the PL spectrum of 1L-WS_2 is well reproduced by the sum of these two peak components, thus the different amount of trion and exciton would lead to different total intensity and position of the PL spectrum. As shown in supporting Figure 2, the PL spectrum extracted from the dark area (weak PL intensity) shows higher trion contribution (low energy PL shoulder) and red-shift compared to the spectrum extracted from the bright area, which should be due to its higher electron density than that of the bright area.

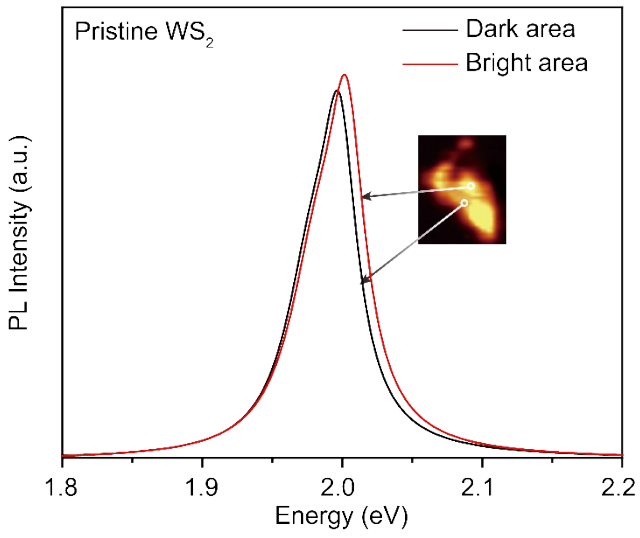

Figure 2. The PL spectra extracted from the bright (red) and dark (black) area of PL mapping (Inset).

Table S1. A brief summary of the PL enhancement in atomically thin transition-metal dichalcogenides (TMDCs).[1-6]

TMDCs	Dopant	PL enhancement factor[a]	References
WS_2	F4TCNQ	~2.3	S1
WS_2	fluorine plasma	~4.2	S2
WS_2	choline plasma	~3.0	S3
MoS_2	F4TCNQ	~3.2	S4
MoS_2	TCNQ	~2.9	S4
MoS_2	graphene	~2.0	S5
MoS_2	gate voltage	~2.8	S6
WS_2	HATCN	~10	This work

[a]The PL enhancement factor is defined as the ratio of the final integrated intensity of modified TMDCs to the integrated intensity of pristine TMDCs.

2. Raman spectra.

The Raman spectra of monolayer WS_2 on SiO_2/Si substrate were conducted through a WITec alpha 300 R system with excitation wavelength of 488 nm.

In order to exclude the strain and defect-induced PL enhancement, we measured the Raman spectra before and after HATCN doping. As shown in Figure S3, the E^1_{2g} peak at ~355 cm^{-1} which is very sensitive to the strain is unchanged, indicating that the strain induced PL enhancement is negligible. Additionally, no defect peak can be observed, which demonstrates that the defect has little influence on the PL enhancement. In contrast, the A_{1g} peak at ~417 cm^{-1} that is very sensitive to the charge density is blue-shift, confirming again the decrease of electron density in monolayer WS_2 owing to the charge transfer from WS_2 to HATCN.[1]

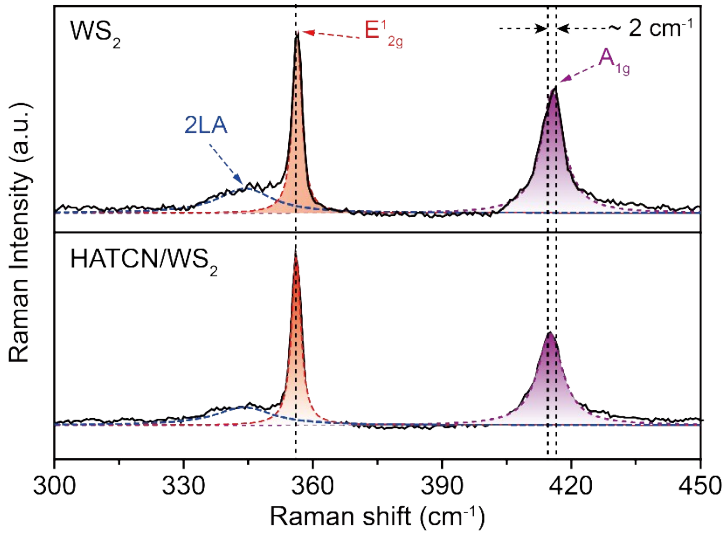

Figure S3. Raman spectra of pristine and HATCN doped monolayer WS_2.

3. The framework of the three-energy-levels

According to the rate equation model [4], the population of neutral excitons (N_X) and trion (N_{X^-}) can be expressed in Equation (S1) and (S2),

$$\frac{dN_X}{dt} = G - \left[\Gamma_{ex} + k_{tr}(n)\right]N_X \tag{S1}$$

$$\frac{dN_{X^-}}{dt} = k_{tr}(n)N_X - \Gamma_{tr}N_{X^-} \tag{S2}$$

where G is the population of excitons after optical excitation, k_{tr}(n) is the generation rate of the trion from the neutral exciton after n-th doping step, Γ_{ex} and Γ_{tr} are the decay rate of neutral exciton and trion, respectively. The experimental values of Γ_{ex} and Γ_{tr} measured from transient absorption measurement are 0.002 and 0.02 ps^{-1}, respectively[7].

The solution of these equations can be written in Equations (4) and (5), respectively,

$$N_X(n) = \frac{G}{\Gamma_{ex} + k_{tr}(n)} \tag{S3}$$

$$N_{X^-}(n) = \frac{k_{tr}(n)}{\Gamma_{tr}} \frac{G}{\Gamma_{ex} + k_{tr}(n)} \tag{S4}$$

Under the assumption that the langmuir's law is valid, k_{tr}(n) can be determined as follows [4],

$$k_{tr}(n) = k_{tr}(0)\left(1 - s\frac{\alpha n\sigma}{1 + \alpha n\sigma}\right) \tag{S5}$$

where α represents a parameter that indicates the HATCN adsorption probability onto the WS_2, n is the doping step, σ is the concentration of HATCN, $k_{tr}(0)$ is the formation rate of pristine monolayer WS_2. The experimental value of $k_{tr}(0)$ obtained from transient absorption measurement is 0.5 ps^{-1}.

According to the previous report, the PL intensity of neutral exciton (I_X) and trion (I_{X^-}) is proportional to the exciton populations, which can be expressed by the following equations

$$I_X(n) = \frac{AG\gamma_{ex}}{\Gamma_{ex} + k_{tr}(n)} \tag{S6}$$

$$I_{X^-}(n) = \frac{k_{tr}(n)}{\Gamma_{tr}} \frac{AG\gamma_{tr}}{\Gamma_{ex} + k_{tr}(n)} \tag{S7}$$

where A is coefficient, γ_{ex} and γ_{tr} are the radiative decay rate of the exciton and trion, respectively. In this calculation, the change of γ_{ex} and γ_{tr} are neglected with doping for simplicity.

4. Mass action model

Under assuming that the mass action law is valid, the relationship among the population of neutral exciton, trion and electron density in monolayer WS_2 can be expressed as [2]

$$\frac{N_X n_{el}}{N_{X^-}} = \left(\frac{4 m_X m_e}{\pi \hbar^2 m_{X^-}} \right) k_B T \exp\left(\frac{E_b}{k_B T} \right) \tag{S8}$$

where $\hbar$ is the reduced Planck's constant, k_B is the Boltzmann constant, T is the temperature, E_b (~26 meV) is the trion binding energy, m_e, m_{X^-} and m_X are electron, trion and exciton effective masses, respectively. m_e and m_h are $0.44m_0$ and $0.45m_0$, where m_0 is a free electron mass[8]. The effective mass of a neutral exciton (m_X) and a trion (m_{X^-}) can be calculated as $m_X = m_e + m_h = 0.89m_0$, $m_{X^-} = 2m_e + m_h = 1.34m_0$, respectively[2].

With Equations S3, S4, S6, S7and S8, the trion PL weight (I_{X^-}/I_{total}) can be determined as

$$\frac{I_{X^-}}{I_{total}} = \frac{\frac{\gamma_{tr}}{\gamma_{ex}} \frac{N_{X^-}}{N_X}}{1 + \frac{\gamma_{tr}}{\gamma_{ex}} \frac{N_{X^-}}{N_X}} \approx \frac{1.65 \times 10^{-14} n_{el}}{1 + 1.65 \times 10^{-14} n_{el}} \tag{S9}$$

The Equation S9 could be used to calculate the electron density n_{el} according to the experimental trion spectra weight.

5. Theoretical calculations

The theoretical calculations were conducted based on the Material Studio2017 Castep module with the GGA/PW91-OBS method.[9] The Generalized Gradient Approximation (GGA) Perdew–Burke–Ernzerhof (PBE) [10] method with Tkatchenko–Scheffler (TS) dispersion correction[11] in CASTEP code with fixed the crystal lattice was used to optimize the geometry. The pseudopotentials are normconserving with a 500 eV energy cutoff. The max force is 0.02, and the max stress is 0.03 GPa, the k-points is 3×3×1. The charge density difference was also calculated by GGA/PBE-TS method in VASP software with the PAW.

Table S2. The calculated charge transfer and absorption energy in chemical doped WS_2.

Dopant	Charge transfer (e)	Absorption energy (eV)
HATCN	-0.18	-1.93
F4TCNQ	-0.09	-1.28

6. Experimental Section

Preparation and characterization of monolayer WS_2. Bulk crystal WS_2 was purchased from HQ Graphene. The monolayer WS_2 flake was conveniently exfoliated from the commercial bulk crystals by the micromechanical method onto a Si wafer with a 280 nm thick SiO_2 capping layer. The optical image was taken by OLYMPUS BX51M. The AFM height image was recorded by Bruker, Dimension Edge.

HATCN doping. HATCN was purchased from HanShang Chemical Scientific Limited. HATCN was dissolved in toluene solution with the concentration of ~2×10^{-5} M. The dopant of HATCN was deposited *via* drop cast method. The volume of one step doping is ~ 10 μL. All of the measurements were performed after the sample dried in ambition condition.

References:

[S1] N. Peimyoo, W. Yang, J. Shang, X. Shen, Y. Wang, T. Yu, *ACS Nano* **2014**, 8, 11320-11329.

[S2] Y. I. Jhon, Y. Kim, J. Park, J. H. Kim, T. Lee, M. Seo, Y. M. Jhon, *Adv. Funct. Mater.* **2016**, 26, 7551-7559.

[S3] Y. Kim, Y. I. Jhon, J. Park, C. Kim, S. Lee, Y. M. Jhon, *Sci. Rep.* **2016**, 6, 21405.

[S4] S. Mouri, Y. Miyauchi, K. Matsuda, *Nano Lett.* **2013**, 13, 5944-5948.

[S5] C. E. Giusca, I. Rungger, V. Panchal, C. Melios, Z. Lin, Y. Lin, E. Kahn, A. L. Elías, J. A. Robinson, M. Terrones, O. Kazakova, *ACS Nano* **2016**, 10, 7840-7846.

[S6] K. F. Mak, K. He, C. Lee, G. H. Lee, J. Hone, T. F. Heinz, J. Shan, *Nat. Mater.* **2012**, 12, 207-211.

[S7] H. Shi, R. Yan, S. Bertolazzi, J. Brivio, B. Gao, A. Kis, D. Jena, H. G. Xing, L. Huang, *ACS Nano* **2013**, 7, 1072-1080.

[S8] A. Ramasubramaniam, *Phys. Rev. B* **2012**, 86, 115409.

[S9] S. J. Clark, M. D. Segall, C. J. Pickard, P. J. Hasnip, M. J. Probert, K. Refson, M. C. Payne, *Z. Kristallogr.* **2005**, 220, 567-570.

[S10] J. P. Perdew, K. Burke, M. Ernzerhof, *Phys. Rev. Lett.* **1996**, 77, 3865-3868.

[S11] M. Scheffler, A. Tkatchenko, *Phys. Rev. Lett.* **2009**, 102, 73005.